This article has been accepted for publication in a future issue of this journal, but has not been fully edited. Content may change prior to final publication. Citation information: DOI 10.1109/TSTE.2018.2869480, IEEE Transactions on Sustainable Energy

Fault-tolerant Economic Model Predictive Control for Wind Turbines

Tushar Jain, *Member, IEEE,* Joseph Julien Yamé, *Member, IEEE*

***Abstract*—The operational cost of wind turbines (WT) is remarkably incurred in fatigue loads induced by torsional vibration within the drive-train subsystem and fore-aft bending of the tower subsystem. Under closed-loop control configuration, actuator faults in pitch subsystem and converter subsystem proliferate these fatigue loads, thereby, severely affect the economic operation of WT. In this paper, we present a novel active fault-tolerant control (FTC) methodology for WT, which minimizes the economic cost of WT by achieving the two broad objectives: power maximization and fatigue reduction, possibly under the effect of torque bias faults in converters. The proposed FTC system is composed of two modules: fault detection and diagnosis (FDD), and controller reconfiguration (CR). We develop the CR module using a model-predictive control (MPC) technique where the primary issue is that the constraint set is not convex in decision variables. The novelty of the proposed scheme lies in transforming the original non-convex optimization problem into a convex problem using some new decision variables. We also develop the FDD module using an unknown-input-residual generator and a *suitably* designed estimation filter to extract the complete information of the fault. This fault information is subsequently used to reconfigure in real-time the constraints of the MPC to ensure system availability. The effectiveness of the developed scheme is demonstrated on a $2MW$ wind turbine system.**

***Index Terms*—Fault-tolerant control, fault diagnosis, renewable energy systems, wind turbines, model-predictive control.**

I. Introduction

THE configuration, technology, and size of wind turbine (WT) systems have been changing rapidly over the last few years with sizeable systems having enhanced energy-capture and economic advantages. Regardless of their striking advantages from the environmental viewpoint, the large, flexible structure of WT systems coupled with working in dynamic wind profile imposes challenges for further reductions in operation and maintenance costs. Under a tight power-wind profile control, the minimization of structural loads requires utmost attention [1], [2]. These structural loads appear due to the flexible nature of the drive-train subsystem, bending of the tower and flapping of the blades exhibiting many vibration modes. In the event of actuator and sensor faults, the closed-loop may excite some of the vibration modes that result in a lifetime reduction or even fatigue breakdown [3]. Moreover, faults in converters and pitch subsystems have a detrimental effect on the required power production from the wind turbine [4]. There is extensive research done in developing fault diagnosis (FD) [5], [6] and fault accommodation subsystems [7], [8], which collectively form the supervision unit [9, Fig. 1.1] within the overall fault-tolerant control (FTC) architecture. These methods use the linearized model of the turbine operating in different regions with respect to a wind profile. An integrated model-based FD-FTC and data-driven FTC scheme have also been investigated in [10] and [11] respectively. On the other hand, classical control strategies for mitigating the structural load in wind turbines under fault-free conditions were studied in [12], [13]. No doubt, the issue of handling the constraints on actuators and sensors using classical control techniques is well-known [2].

In order to address the multi-objective performance, i.e., maximizing power and alleviating structural load together with handling the constraints on system variables, model predictive control (MPC) techniques were developed in [14], [15] utilizing the linearized model of the wind turbine. The MPC techniques utilizing the nonlinear model of the turbine were also developed in [16], [17]. However, the real-time deployment issues of these nonlinear MPC techniques is a major concern due to several factors [17, Section 5.3] such as solving a non-convex optimization problem, computational effort required, etc. These concerns may restrict their integration to develop further a real-time (active) FTC system because of the following reasons: (a) FTC guarantees a fail-safe system, which requires a fast solution of the control inputs; (b) due to heavy dependency on naturally generated wind supply, the linear models used in MPC (i.e., in the control execution unit) need to be recomputed for changing operating conditions or a bank of linear models is required [18]; (c) highly reduced non-linear model of the turbine might be used for designing an MPC controller [16], however, they might not be suitable for fault diagnosis (i.e. in the supervision unit) that extracts the precise information about the fault. Apparently, due to these limitations, no work has been reported in the literature with non-linear MPC in the control execution unit of the FTC architecture. Numerous developed FTC approaches based on MPC for wind turbines use the linearized model of the turbine around some operating point [19].

To address the above issues, we present a novel fault-tolerant control strategy for bias faults in converter subsystem of wind turbines. Our main contributions are: first, from insights into the original non-linear model of the wind turbine, we formulate a time-derivative energy model incorporating the flexible structure of the tower and drive-train subsystems which is completely equivalent to the non-linear model. This transformed equivalent model facilitates a convex reformula-

Tushar Jain is with School of Computing and Electrical Engineering, Indian Institute of Technology Mandi, Kamand 175005, Himachal Pradesh, India e-mail: (tushar@iitmandi.ac.in)

Joseph J. Yamé is with Centre de Recherche en Automatique de Nancy, CRAN-CNRS, Université de Lorraine, BP 70239 - 54506 Nancy, France e-mail: (joseph.yame@univ-lorraine.fr)

This article has been accepted for publication in a future issue of this journal, but has not been fully edited. Content may change prior to final publication. Citation information: DOI 10.1109/TSTE.2018.2869480, IEEE Transactions on Sustainable Energy

tion of the original non-convex economic optimization problem for model predictive control of wind turbines. Secondly, a model-based fault detection and estimation algorithm is developed, which utilizes a Taylorian linearized model of the turbine around an equilibrium point to extract the complete information about the bias fault. This algorithm is based on an unknown input residual generator (UIRG) and on a specifically designed filter for estimating bias fault in converter subsystem of wind turbines . The complete knowledge about the fault is then used for online updating of the constraints of the predictive controller thereby ensuring the system dependability.

II. Wind turbine model and problem formulation

A. Dynamics of the turbine

The overall wind turbine system is composed of the aerodynamic rotor subsystem, flexible drive-train shaft subsystem, generator, and flexible tower subsystem. The total power in the wind, computed from the kinetic energy stored in the wind, is given by $P_w(t) = \frac{1}{2}\rho A v_a^3(t)$, where ρ is the air density, A is the transversal area, v_a is the apparent wind speed. The blades of the wind turbines are specifically designed to convert a part of the kinetic energy of the wind into useful mechanical energy. Using the actuator disc theory, a theoretical upper-bound to the energy conversion efficiency is computed, which is expressed by the non-dimensional power coefficient C_p, defined as the ratio of extracted power to wind power

$$C_p = \frac{P_r}{P_w}, \tag{1}$$

where P_r denotes the power extracted from the wind and absorbed by the rotor [3]. For variable-pitch wind turbines, the coefficient C_p is a function of the blade pitch angle $\beta(t)$, which must satisfy the constraint

$$\beta_{min} \leq \beta(t) \leq \beta_{max}, \tag{2}$$

and the blade tip speed ratio, given by $\lambda(t) \propto \frac{\omega_r(t)}{v_a(t)}$, where $\omega_r(t)$ is the rotor angular velocity, which is also restricted within the bounds:

$$\omega_{r,min} \leq \omega_r(t) \leq \omega_{r,max}. \tag{3}$$

This functional coefficient C_p is determined by solving the blade element momentum equation, and the numerical solution is provided in a look-up table [3]. Thus, from (1) the mechanical aerodynamics power captured by the rotor is given by $P_r(t) = P_w(t)C_p(\lambda(t), \beta(t)) = \frac{1}{2}\rho A C_p(\lambda(t), \beta(t)) v_a^3(t)$. The mechanical energy exerts a torque on the rotor, given by

$$T_r(t) = \frac{P_r(t)}{\omega_r(t)} = \frac{1}{2\omega_r(t)}\rho A C_p(\lambda(t), \beta(t)) v_a^3(t). \tag{4}$$

The aerodynamic torque is then transferred to the generator through the *flexible* drive-train subsystem, which includes the gearbox, low-speed shaft and high-speed shaft. Conceptually, the drive-train system is arranged into several rigid bodies linked by flexible joints, which determines the order of the model. This arrangement yields high order nonlinear models [20]. For practical purposes, it is sufficient to include in the model just one or two degrees of freedom in the plane of rotation that are directly coupled to the control [3, Chapter 3]. Therefore, the drive-train is described by a two-mass model, where the gearbox is modeled as a rigid body and the flexibility is considered by a torsion spring on the low-speed shaft. The dynamics of the drive-train system is given by following first-order linear differential equations

$$J_r\dot{\omega}_r(t) = T_r(t) - T_{ls}(t), \qquad T_{ls}(t) = K_{dt}\theta_{dt}(t), \tag{5a}$$

$$J_g\dot{\omega}_g(t) = T_{hs}(t) - T_g(t), \qquad T_{hs}(t) = \frac{T_{ls}(t)}{N_g}, \tag{5b}$$

$$\dot{\theta}_{dt}(t) = \omega_r(t) - \frac{\omega_g(t)}{N_g}, \tag{5c}$$

where the parameters J_r and J_g represents the combined inertia at the rotor side and generator side respectively, K_{dt} represents the torsion stiffness of the rotor with the gear ratio N_g, $\theta_{dt}(t)$ is the torsion angle of the drive-train, $T_{ls}(t)$ denotes the low-speed shaft torque, $T_{hs}(t)$ denotes the high-speed shaft torque, and $\omega_g(t)$ and $T_g(t)$ denotes the generator angular velocity and torque respectively satisfying the following bounds:

$$\omega_{g,min} \leq \omega_g(t) \leq \omega_{g,max}, \tag{6}$$

$$0 \leq T_g(t) \leq T_{g,max}. \tag{7}$$

The generator impose an electrical counter torque on the drive shaft and thereby extract the electrical power, $P_g(t)$, given by

$$P_g(t) = \eta_g T_g(t)\omega_g(t), \tag{8}$$

where $\eta_g \in [0, 1]$ is the generator efficiency. This power is constrained by

$$P_{min} \leq P_g(t) \leq P_{rated}, \tag{9}$$

where P_{rated} is the rated generator power.

The wind speed exerts a thrust on the rotor inducing vibration in the flexible tower of the turbine is known as tower fore-aft bending. Here, we consider only its first mode. The total force of the wind on the actuator disc model is given by $F_w(t) = \frac{1}{2}\rho A v_a^2(t)$. The thrust force acts on the turbine blades and depends on the blade aerodynamics, by another dimensionless quantity, thrust coefficient C_t, which is also a function of $\lambda(t)$ and $\beta(t)$, determined by solving the blade element momentum equation, and the numerical solution is provided in a look-up table [3]. Consequently, the thrust force on the rotor is given by

$$F_t(t) = F_w(t)C_t(\lambda(t), \beta(t)) = \frac{1}{2}\rho A C_t(\lambda(t), \beta(t)) v_a^2(t).$$

The tower fore-aft motion is modeled by a mass, spring, and damper system, i.e.

$$M_t\ddot{x}_t(t) + B_t\dot{x}_t(t) + K_t x_t(t) = F_t(t), \tag{10}$$

where B_t is the tower damping coefficient, K_t is the tower torsion coefficient, M_t is the top mass of the tower, and $x_t(t)$ denotes the displacement of the nacelle from its equilibrium position. This fore-aft motion affects the effective wind speed on the rotor, which yields the apparent wind speed, $v_a(t)$

$$v_a(t) = v_w(t) - \dot{x}_t(t),$$

This article has been accepted for publication in a future issue of this journal, but has not been fully edited. Content may change prior to final publication. Citation information: DOI 10.1109/TSTE.2018.2869480, IEEE Transactions on Sustainable Energy

where $v_w(t)$ is the mean wind speed and $\dot{x}_t(t)$ denotes the tower-top speed. With the hub height h_H, the tower base fore-aft bending moment (TFAM) M_{yT} is given by [17]

$$M_{yT} = h_H(B_t\dot{x}_t(t) + K_t x_t(t)) \tag{11}$$

On the system level, the actuator is the converter of the power system within the wind turbine. Its role is to load the generator producing the electric power with a certain torque. The converter dynamics can be modeled by a first-order differential equation [4]

$$\dot{T}_g(t) = -\frac{1}{\kappa}T_g(t) + \frac{1}{\kappa}T_{g,ref}(t), \tag{12}$$

where $T_{g,ref}(t)$ is the reference command for the generator torque and κ denotes the converter model parameter. Finally, the overall WT dynamics including the actuator subsystem is fully described by the set of differential equations (5), (10) and (12). Defining the state $x(t)$, control $u(t)$, and disturbance $d(t)$, as

$$\begin{aligned} x(t) &= \begin{bmatrix} T_g(t) & \omega_r(t) & \omega_g(t) & \theta_{dt}(t) & x_t(t) & \dot{x}_t(t) \end{bmatrix}^T, \\ u(t) &= \begin{bmatrix} T_{g,ref}(t) & \beta(t) \end{bmatrix}^T, \\ d(t) &= v_w(t), \end{aligned} \tag{13}$$

the WT dynamics can be written in state-space form

$$\dot{x}(t) = \psi(x, u, d) \tag{14}$$

with $\psi(x, u, d)$ denoting the resulting non-linear vector-valued function of the state equations.

B. Fault modelling

A detailed description of different types of frequently occurring faults, which can result in unsatisfactory control performance is discussed in [4]. Among them, torque bias faults in the converter, classified into actuator faults, originate from either an internal fault in the converter electronics or a bias in the converter torque estimate which itself can be due to design/manufacturing defects. Typically, the converter internal controller is able to detect and accommodate the faults in electronics, however addressing the torque bias imposes challenges [4]. Here, we consider the bias fault in converter, which changes the input to the plant to

$$u_f(t) = u(t) + f(t), \tag{15}$$

where $f(t) = \begin{bmatrix} T_b & 0 \end{bmatrix}^T$ and T_b is the bias. Note that from (8), the converter torque can be expressed as the ratio of generated power and angular speed of the generator, i.e. $T_g(t) = \eta_g \times (P_g(t)/\omega_g(t))$. Due to this, an occurrence of torque bias fault may cause unexpected overshoots and fluctuations in the turbine dynamics and in the generated power. Since the tower fore-aft motion is excited by the forcing function $F_t(t)$ which is a nonlinear function of the angular speed, the bias fault in turn induces higher fatigue loads, which is analyzed by computing the TFAM (11). As a consequence, the bias fault in converter dynamics drastically impact the power quality in the electrical grid codes and results in reducing the WT lifetime due to alleviation in structural loads [21], [22].

C. Problem formulation

The problem we aim to solve is to control the wind turbine in order to maximize the energy production without damages which might be caused by severe structural loads acting on the tower. This objective should be also enforced under WT actuator faults to ensure the dependability of the overall system. To deal with the constraints on system input and output signals, the above control problem is mathematically formulated within a receding horizon optimal control framework. The control problem is therefore posed as

$$\min_u J = \int_{t_0}^{t_0+T_f} \ell(x(\tau), u(\tau), d(\tau))d\tau \tag{16a}$$

$$\text{s.t. } (14) \tag{16b}$$

$$x(t_0) = x_0 \tag{16c}$$

$$(2), (3), (6), (9) \ \ \forall \tau \in [t_0, t_0 + T_f] \tag{16d}$$

with the instantaneous cost given by

$$\begin{aligned} \ell(x, u, d) = &-\alpha_1 P_r + \alpha_2 \dot{P}_g^2 + \alpha_3 \dot{P}_r^{\,2} \\ &+ \alpha_4 \dot{F}_t^{\,2} + \alpha_5 \dot{x}_t^{\,2} + \alpha_6 (K_r - K_r^{ref})^2, \end{aligned} \tag{17}$$

where

$$K_r(t) = \frac{1}{2} J_r \omega_r^2(t) \tag{18}$$

is the kinetic energy of the rotor and $\alpha_i, i \in \{1, 2, 3, 4, 5, 6\}$ are positive constants. The rationale behind the choice of the instantaneous cost is the following: the first term aims at maximizing the rotor power captured from the available wind power thereby maximizing the WT generated power. The second term aims at minimizing the variations of the generated power. The third and fourth term aim at minimizing the variations of rotor power and thrust force respectively. The fifth term relates to the tower fore-aft velocity which should be minimized to reduce the structural loads acting on the tower. The last term aims at minimizing the deviation of the kinetic energy from its reference value K_r^{ref}. Clearly, the objective is essentially an economic performance goal to be achieved with a damage-aware control strategy for improving the wind turbine lifetime aiming ultimately at maximizing the system profitability. Though the functional in (16a) is a convex function of the quantities $-P_r, P_g, \dot{F}_t, \dot{x}_t$ and K_r, it is not a convex function of the decision variables u, x given by (13) and moreover, the constraint set is not a convex set of the decision variables. Consequently, the economic model predictive control (eMPC) problem (16) is a highly nonlinear and non-convex optimization problem.

Our global objective is to design an optimal active fault-tolerant control (FTC) scheme based on the above economic performance goal under the possible occurrences of bias faults in the WT converter subsystem. The main non-trivial issues to be solved for this optimal FTC problem are therefore:

- How to diagnose the bias fault in the converter?
- How to solve the non-convex control optimization problem (16)?

This article has been accepted for publication in a future issue of this journal, but has not been fully edited. Content may change prior to final publication. Citation information: DOI 10.1109/TSTE.2018.2869480, IEEE Transactions on Sustainable Energy

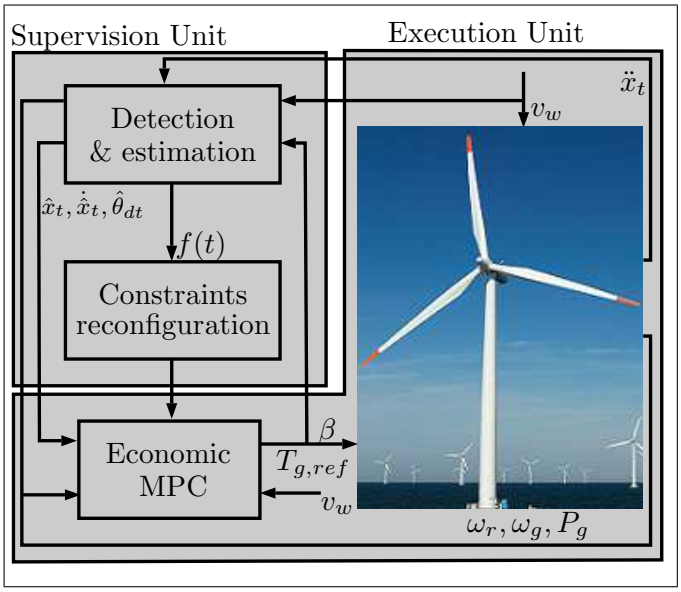

Fig. 1. Structure of the fault-tolerant control scheme of wind turbines

III. Fault-tolerant Economic Model Predictive Control

In this section, we present the detailed solution to the optimal fault-tolerant economic model predictive control (FTeMPC) problem stated in the previous subsection. This FTeMPC scheme is realized through the integration of a specific fault detection and diagnosis (FDD) algorithm able to estimate quickly the fault signal and a model predictive controller solving the optimization problem (16). The overall structure of the proposed FTeMPC system for wind turbines is illustrated in Fig. 1.

A. Fault diagnosis system for WT converters

To build the FDD algorithm, the nonlinear WT dynamics (14) is linearized around the operating point (x^*, u^*, d^*) and then discretized with a sampling period h, leading to

$$\begin{aligned} x(k+1) &= Ax(k) + B_u u(k) + b_d d(k) \\ y(k) &= Cx(k) + Du(k) + d_d d(k), \end{aligned} \tag{19}$$

where $A, B_u, C, D,$ and b_d, d_d are the resulting discrete-time system matrices and vectors of appropriate dimensions respectively. The vector $y = \begin{bmatrix} a_t & \omega_g & \omega_r & P_g \end{bmatrix}^T$, with a_t denoting the tower-top acceleration, is the system output. In order to avoid cumbersome notations, the signals in (19) now denote small variations around their operating values. Under the event of bias fault in converter, the state equation reads

$$x(k+1) = Ax(k) + B_u u(k) + B_f f(k) + b_d d(k),$$

with $B_f = B_u$ and the signal $f(k)$ contains the information of the bias fault. Note that $u(k)$ is the output of the controller and under fault-free scenario it is also the input to the WT plant, while $u(k) + f(k) \triangleq u_f(k)$ with $f(k) = \begin{bmatrix} T_b & 0 \end{bmatrix}^T$ denotes the actual input to the WT plant under the event of bias fault in converters. For fault diagnosis, the first step is to detect and isolate the occurred fault. This is achieved here by designing an unknown input residual generator (UIRG) specifically for handling the converter faults. Before designing the UIRG, we reduce the linear state-space model from a 6-state model to a 2-state model using (5). Writing (19) explicitly, the linearized model is obtained as

$$\begin{aligned} \begin{bmatrix} x_1(k+1) \\ x_2(k+1) \end{bmatrix} &= \begin{bmatrix} A_1 & \mathbf{0}_{4\times 2} \\ A_2 & A_3 \end{bmatrix} \begin{bmatrix} x_1(k) \\ x_2(k) \end{bmatrix} + B_u u(k) + b_d d(k) \\ \begin{bmatrix} y_1(k) \\ y_2(k) \end{bmatrix} &= \begin{bmatrix} C_{11} & C_{12} \\ C_{21} & \mathbf{0}_{3\times 2} \end{bmatrix} \begin{bmatrix} x_1(k) \\ x_2(k) \end{bmatrix} \\ &\quad + \begin{bmatrix} 0 & d_{12} \\ \mathbf{0}_{3\times 1} & \mathbf{0}_{3\times 1} \end{bmatrix} \begin{bmatrix} u_1(k) \\ u_2(k) \end{bmatrix} + \begin{bmatrix} d_1 \\ \mathbf{0}_{3\times 1} \end{bmatrix} d(k), \end{aligned}$$

where $\mathbf{0}_\bullet$ denotes the zero matrix of appropriate dimension, $x = \begin{bmatrix} x_1 & x_2 \end{bmatrix}^T$ with $x_1 = \begin{bmatrix} T_g & \omega_r & \omega_g & \theta_{dt} \end{bmatrix}^T$, $x_2 = \begin{bmatrix} x_t & v_t \end{bmatrix}^T$, where v_t is the tower-top velocity, $y = \begin{bmatrix} y_1 & y_2 \end{bmatrix}^T$ with $y_1 = a_t$, $y_2 = \begin{bmatrix} \omega_g & \omega_r & P_g \end{bmatrix}^T$, and $u = \begin{bmatrix} u_1 & u_2 \end{bmatrix}^T = \begin{bmatrix} T_{g,ref} & \beta \end{bmatrix}^T$. It is worth noticing that the state x_1 and the output y_2 are not influenced by x_2. In addition, neither x_2 nor y_1 are directly affected by the control input signal u_1. The state-space model with 4-states and having the similar dynamics as of (19) is then written as

$$\begin{aligned} x_1(k+1) &= A_1 x_1(k) + \tilde{B}_u u(k) + \tilde{b}_d d(k) \\ y_2(k) &= C_{21} x_1(k) \end{aligned} \tag{20}$$

where $\tilde{B}_u$ and $\tilde{b}_d$ are easily obtained from the associated matrices of the aforementioned state-space model. We further analyzed this model at steady state where the signal θ_{dt} is close to zero and its time-derivative shows small variations around zero. Simplifying (5) using the aforementioned analysis and then discretizing with a sampling period h yields, from (20), the following reduced-order model

$$\begin{aligned} \breve{x}(k+1) &= \breve{A}\breve{x}(k) + \breve{B}_u u(k) + \breve{b}_d d(k) \\ \breve{y}(k) &= \breve{C}\breve{x}(k) \end{aligned} \tag{21}$$

where $\breve{x} = \begin{bmatrix} \omega_g & T_g \end{bmatrix}^T, \breve{y} = \begin{bmatrix} \omega_g & P_g \end{bmatrix}^T$, and matrices $\breve{A}, \breve{B}_u, \breve{b}_d, \breve{C}$ are of appropriate dimension. Under the event of bias fault in converter, the state equation now reads

$$\breve{x}(k+1) = \breve{A}\breve{x}(k) + \breve{B}_u u(k) + \breve{B}_f f(k) + \breve{b}_d d(k)$$

with $\breve{B}_f = \breve{B}_u$. We use the 2-state model (21) for fault diagnosis in converters.

Consider the nominal (fault-free) dynamics of the WT system written as

$$\breve{x}(k+1) = \breve{A}\breve{x}(k) + \breve{B}_\nu \nu(k) + \breve{b}_{u_2} u_2(k),$$

where the vector $\nu(k)$ is defined by $\nu = \begin{bmatrix} u_1(k) & d(k) \end{bmatrix}^T$, and the matrix $\breve{B}_\nu = \begin{bmatrix} \breve{b}_{u_1} & \breve{b}_d \end{bmatrix}$. The signal $u_2(k)$ is now viewed as the only unknown input. For detecting the bias fault in converter subsystem, the UIRG is constructed as [23]

$$\begin{aligned} z(k+1) &= Fz(k) + T\breve{B}_\nu \nu(k) + K\breve{y}(k) \\ r(k) &= \left(\mathbf{I} - \breve{C}H\right)\breve{y}(k) - \breve{C}z(k), \end{aligned} \tag{22}$$

This article has been accepted for publication in a future issue of this journal, but has not been fully edited. Content may change prior to final publication. Citation information: DOI 10.1109/TSTE.2018.2869480, IEEE Transactions on Sustainable Energy

where the matrices F, T, K, H are the parameters computed as

$$\begin{aligned} H &= \breve{b}_{u_2}\left(\left(\breve{C}\breve{b}_{u_2}\right)^T \breve{C}\breve{b}_{u_2}\right)^{-1}\left(\breve{C}\breve{b}_{u_2}\right)^T \\ T &= \mathbf{I} - H\breve{C} \\ F &= T\breve{A} - \bar{K}\breve{C} \\ K &= \bar{K} + FH \end{aligned} \tag{23}$$

with the parameter $\bar{K}$ chosen such that F is a stable matrix. The necessary and sufficient conditions for the existence of the UIRG (22, 23) are given by [23, Theorem 3.1], i.e.

1) $\texttt{rank}\left(\breve{C}\breve{b}_{u_2}\right) = \texttt{rank}\left(\breve{b}_{u_2}\right)$,
2) $\left(T\breve{A}, \breve{C}\right)$ is detectable.

It turns out that the pair $(T\breve{A}, \breve{C})$ satisfies the stronger property of being observable. The detection and isolation logic under a fault-free converter or a bias in converter dynamics is then given by

$$\begin{aligned} \|r(k)\| &< th \quad \text{for fault-free case} \\ \|r(k)\| &\geq th \quad \text{for faulty case} \end{aligned} \tag{24}$$

where th is a given threshold value. To achieve the complete fault diagnosis, an estimation of the bias is required. Consider again the filter (22) with the explicit control and disturbance signals, however, instead of the control signal $u_1(k)$ we use the actual input to the WT plant, i.e. $u_{1,f}(k)$

$$\begin{aligned} \varsigma(k+1) &= F\varsigma(k) + T\breve{b}_{u_1}u_{1,f}(k) + T\breve{b}_d d(k) + K\breve{y}(k) \\ \varrho(k) &= \left(\mathbf{I} - \breve{C}H\right)\breve{y}(k) - \breve{C}\varsigma(k). \end{aligned} \tag{25}$$

Clearly, with the faulty input $u_{1,f}(k)$, the residual $\varrho(k)$ in the filter (25) is actually equal to zero. Moreover, under fault-free scenario the filters (22) and (25) are completely *equivalent*. From $\varrho(k) = 0$, we have $(\mathbf{I} - \breve{C}H)\breve{y}(k) = \breve{C}\varsigma(k)$. The matrix $\breve{C}$ is invertible and $u_{1,f}(k) = u_1(k) + T_b$, it results that all signals in (25) are available, except $f(k)$. The matrix $T\breve{b}_{u_1}$ is of full column rank, so the bias in the converter can be estimated by solving an inverse-type algebraic problem. Let $T\breve{b}_{u_1} = U\begin{bmatrix}\sigma \\ 0\end{bmatrix}1$ be the singular value decomposition (SVD) of the matrix $T\breve{b}_{u_1}$, where the singular value σ is a strict positive scalar, and U is an orthonormal matrix. Using the SVD and substituting it in (25) leads to the following algebraic computation of the bias fault

$$\begin{aligned} \hat{T}_b = \frac{1}{\sigma}\begin{bmatrix}1 & 0\end{bmatrix} \times \left\{\hat{\varsigma}(k+1) - \bar{F}\hat{\varsigma}(k) - \bar{b}d(k) - \bar{K}y(k)\right\} \\ - u_1(k) \end{aligned} \tag{26}$$

where $\hat{\varsigma}(k) = U^T\varsigma(k), \bar{F} = U^TFU, \bar{b} = U^T T\breve{b}_d$, and $\bar{K} = U^TK$. The estimation of the bias fault is triggered whenever a fault is detected by the fault detection system (24). If k denotes the time at which the bias is estimated using (26), then the fault may have occurred at or before time $k-1$. Since the bias fault is a constant signal, formula (26) uses the signals available up to time k. Thanks to the nullity of the residual $\varrho(k)$ and the matrix $\breve{C}$ being invertible, the estimation provided at time k by (26) is equivalently given by

$$\begin{aligned} \hat{T}_b = \frac{1}{\sigma}\begin{bmatrix}1 & 0\end{bmatrix} \times \\ \begin{bmatrix}\breve{C}^{-1}(\mathbf{I} - \breve{C}H) & -\bar{F}\breve{C}^{-1}(\mathbf{I} - \breve{C}H) - \bar{K} & -\bar{b}\end{bmatrix}\begin{bmatrix}\breve{y}(k) \\ \breve{y}(k-1) \\ d(k-1)\end{bmatrix} \\ - u_1(k-1) \end{aligned} \tag{27}$$

The full FDD of WT bias faults in converters is achieved in two sequential steps:

1) Fault detection (FD) performed by the UIRG (22), (23), (24)
2) Bias-fault estimation triggered by the FD stage and performed by filter (27).

B. Economic Model Predictive Control

As mentioned earlier, the eMPC problem (16) is a highly non-linear and non-convex problem since the constraint set of the decision variables of this problem is not naturally a convex set. The angle of attack of the problem is to reformulate the eMPC optimization problem as an equivalent convex optimization problem through some judicious choice of new decision variables. These new decision variables are exhibited naturally through a particular representation of the wind turbine dynamics as a linear dynamics which turns out to bear the *same behavior* as the nonlinear dynamics (14). This representation stems from the instantaneous total energy stored in the rotational motion of the drive train given by

$$K(t) = K_r(t) + K_g(t) + K_{\theta_{dt}}(t). \tag{28}$$

where $K_r(t)$ is the instantaneous kinetic energy in the rotor defined by (18), $K_g(t) = \frac{1}{2}J_g\omega_g^2(t)$, the kinetic energy in the generator, and $K_{\theta_{dt}}(t) = \frac{1}{2}K_{dt}\theta_{dt}^2(t)$, the potential energy in the flexible shaft. Thanks to (5c), the time-derivative of the total energy, after further simplifications using (5), can be written as

$$\dot{K}(t) = T_r(t)\omega_r(t) - T_g(t)\omega_g(t) \tag{29}$$

with $T_g(t)$ given by (12). Therefore, using (4) and (8), equation (29) reads as

$$\dot{K}(t) = P_r(t) - \frac{1}{\eta_g}P_g(t). \tag{30}$$

The drive train dynamics (30) and the tower dynamics (10) can be lumped together into the following linear state-space system

$$\begin{bmatrix}\dot{K} \\ \dot{x}_t \\ \ddot{x}_t\end{bmatrix} = \begin{bmatrix}0 & 0 & 0 \\ 0 & 0 & 1 \\ 0 & -\frac{K_t}{M_t} & -\frac{B_t}{M_t}\end{bmatrix}\begin{bmatrix}K \\ x_t \\ \dot{x}_t\end{bmatrix} + \begin{bmatrix}1 & -\frac{1}{\eta_g} & 0 \\ 0 & 0 & 0 \\ 0 & 0 & \frac{1}{M_t}\end{bmatrix}\begin{bmatrix}P_r \\ P_g \\ F_t\end{bmatrix}, \tag{31}$$

with the following new state and control variables

$$\underline{x}(t) = \begin{bmatrix}K(t) & x_t(t) & \dot{x}_t(t)\end{bmatrix}^T, \tag{32a}$$

$$\underline{u}(t) = \begin{bmatrix}P_r(t) & P_g(t) & F_t(t)\end{bmatrix}^T \tag{32b}$$

This article has been accepted for publication in a future issue of this journal, but has not been fully edited. Content may change prior to final publication. Citation information: DOI 10.1109/TSTE.2018.2869480, IEEE Transactions on Sustainable Energy

Now, with these new variables, the constraints on angular speeds can be expressed as constraints on kinetic energy as

$$(J_r/2)\omega_{r,min}^2 \leq K_r(t) \leq (J_r/2)\omega_{r,max}^2, \tag{33a}$$
$$(J_g/2)\omega_{g,min}^2 \leq K_g(t) \leq (J_g/2)\omega_{g,max}^2. \tag{33b}$$

From (8), the generator torque constraints can be translated into

$$0 \leq P_g(t) \leq \eta_g \sqrt{(2/J_g)K_g(t)}T_{g,max}. \tag{34}$$

Observe that constraint (34) is a convex set with regards to variables P_g and K_g since minus the square root of K_g is convex and for constraint (33), it is obvious that the set it defines is trivially a convex set of the variables K_r, K_g.

Introduce the available wind power P_{av} given by [3], [24]

$$P_{av}(\lambda(t)) = \max_{\beta_{min}\leq\beta(t)\leq\beta_{max}} P_w(t)C_p(\lambda(t),\beta(t)).$$

The power coefficient $C_p(\lambda(t),\beta(t))$ can be expressed as $C_p(v_a(t),\sqrt{(2/J_r)K_r(t)},\beta(t))$ using (18). Thus,

$$P_{av}(v_a,K_r) = \max_{\beta_{min}\leq\beta\leq\beta_{max}} \frac{1}{2}\rho A C_p(v_a,K_r,\beta)v_a^3. \tag{35}$$

From (1), we know that (35) provides an upper bound on the captured wind power, i.e.

$$P_r(t) \leq P_{av}(v_a(t),K_r(t)). \tag{36}$$

The exerted wind force F_{ex} defined as

$$F_{ex}(\lambda(t)) = \max_{\beta_{min}\leq\beta(t)\leq\beta_{max}} F_w(t)C_t(\lambda(t),\beta(t)) \tag{37}$$

can also be seen as a function of wind speed, tower-top velocity and the kinetic energy, i.e.,

$$F_{ex}(v_a,K_r) = \phi_{v_w,\dot{x}_t}(K_r)\, v_a^2 \tag{38}$$

with

$$\phi_{v_w,\dot{x}_t}(K_r) = \max_{\beta_{min}\leq\beta\leq\beta_{max}} \frac{1}{2}\rho A C_t(v_w,\dot{x_t},K_r,\beta) \tag{39}$$

As the thrust force cannot exceed the exerted wind force, this yields the constraint

$$0 \leq F_t(t) \leq F_{ex}(v_w(t),\dot{x_t}(t),K_r(t)). \tag{40}$$

Thanks to the new decision variables $\underline{u}$, $\underline{x}$, the eMPC problem reads as

$$\min_{\underline{u}} J = \int_{t_0}^{t_0+T_f} \ell(\underline{x}(\tau),\underline{u}(\tau),v_w(\tau))d\tau \tag{41a}$$
$$\text{s.t. } (31) \tag{41b}$$
$$\underline{x}(t_0) = \underline{x}_0 \tag{41c}$$
$$(33),(34),(36),(40) \ \ \forall\tau\in[t_0,t_0+T_f] \tag{41d}$$

where we have explicitly shown the dependence of the instantaneous cost (17) in terms of the new decision variables (32). Clearly, the instantaneous cost $\ell(\underline{x},\underline{u},v_w)$ is now a convex function of the decision variables $\underline{x},\underline{u}$. However, the optimization problem (41) is still non-convex because of the constraint sets (36), (40). If we assume that the wind speed is nearly constant then the tower-top acceleration is approximately close to zero and yields a constant tower-top velocity. Under this assumption, the ϕ-function defined in (39) has only K_r as argument and consequently the exerted force can be seen as a function of K_r parametrized by v_a, i.e.,

$$F_{ex}(v_a,K_r) = \phi(K_r)\, v_a^2 \tag{42}$$

The function (42) is drawn in Fig. 2 with $K_r(t)$ as the independent variable and the apparent speed v_a as a parameter. This shows that the function $\phi(K_r)$ is a quasi-concave function of $K_r(t)$ and therefore it can be approximated closely by a concave function. Let denote this concave approximation by $\hat{\phi}(K_r)$, then it can be represented as the infimum of an affine family referenced by means of a counting set $\sigma = 1,2,...,p$, $p \leq \infty$ (see [25], [26])

$$\hat{\phi}(K_r) = \inf_{k\in\sigma}\{\alpha_k K_r + \gamma_k\}$$

For each 'parameter' $v_{a,i}$, with i belonging to a finite counting set, the concave approximation $\hat{F}_{ex}(v_{a,i},K_r) = \hat{\phi}(K_r)\, v_{a,i}^2$ holds and for any given $v_{a,m}$ and $v_{a,n}$ such that $v_{a,m} \leq v_a \leq v_{a,n}$, the exerted force at v_a can be approximated by a linear interpolation

$$\hat{F}_{ex}(v_a,K_r) = (1-\chi)\hat{F}_{ex}(v_{a,m},K_r) + \chi\hat{F}_{ex}(v_{a,n},K_r)$$

with $\chi = \frac{v_a - v_{a,m}}{v_{a,n}-v_{a,m}}$. Consequently, the constraint (40) in the optimization problem (41) is approximated by the following constraint

$$0 \leq F_t(t) \leq \hat{F}_{ex}(v_a(t),K_r(t)). \tag{43}$$

which is a convex set with regards to $F_t(t)$ and $K_r(t)$.A similar approximation technique is used for constraint (36) whereby allowing the non-convex optimal control problem to be approximated by a convex optimization problem.

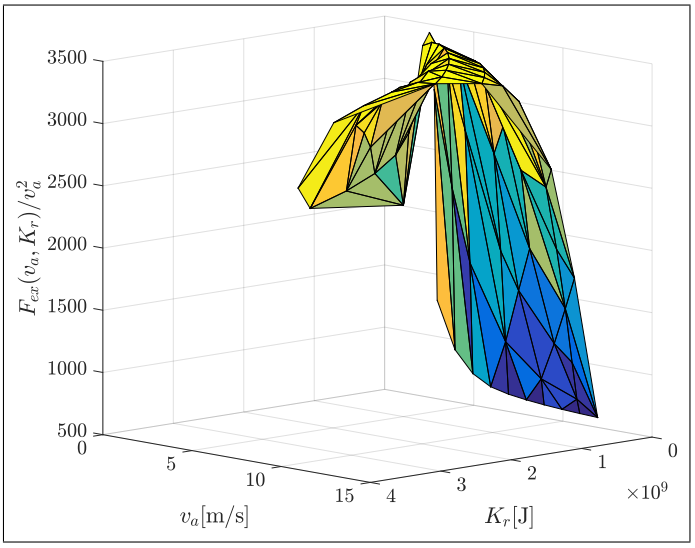

Fig. 2. $F_{ex}(v_a,K_r)$ normalized by v_a^2 curve plotted using the NREL's benchmark wind turbine system

C. Implementation of the FTeMPC

In the above eMPC optimization problem, the information about wind velocity is assumed to be known for prediction. The measured variables in the closed-loop, i.e. ω_r, ω_g, P_g,

This article has been accepted for publication in a future issue of this journal, but has not been fully edited. Content may change prior to final publication. Citation information: DOI 10.1109/TSTE.2018.2869480, IEEE Transactions on Sustainable Energy

are shown in Fig. 1. Consequently, with the linear dynamics (5), the state $K(t)$ of system (31) can be computed. The states $x_t(t)$ and $\dot{x}_t(t)$ are not measurable, an estimator is therefore used to estimate the states $x_t(t)$ and $\dot{x}_t(t)$ (see, e.g., [17]). However, the tower top acceleration $\ddot{x}(t)$ is directly measurable. Since $u(t) = \begin{bmatrix} T_{g,ref}(t) & \beta(t) \end{bmatrix}^T$ is the actual control variable, $\beta(t)$ is determined inversely as a function $\Phi_\beta(v_a, K_r, P_r, F_t)$ that gives the captured power P_r and the thrust force F_t. Similarly, the value of $T_{g,ref}(t)$ is extracted using a function $\Phi_{T_{g,ref}}(K_g, P_g)$ that gives the generated power P_g.

To implement the continuous time eMPC, the cost functional in (41a) is approximated through numerical integration by using values of $\ell(\underline{x}(\tau), \underline{u}(\tau), v_w(\tau))$ at equidistant time-points $\tau_k, k = 0, 1, \ldots, N_p$, with $\tau_k = t_0 + kh$ where h is the sampling period used in discretizing the linearized model in section III-A and $T_f = N_p h$. Using the values of the continuous-time signals $\underline{x}$ and $\underline{u}$ at the grid points τ_k, the integral J over the horizon is approximated by the rectangle rule, i.e., $J_{N_p} = \sum_{k=0}^{N_p-1} \ell_k(\underline{x}(k), \underline{u}(k), v_w(k))h$. The time derivative of the state vector in (41b) is approximated by Euler method [27].

Under the event of bias fault, the generated power P_g, computed using (8), changes from the nominal mode or healthy mode to the faulty mode because of its dependence on the actual control variable, $T_{g,ref}$. The constrained optimization might become infeasible due to the inequality constraints (41d). To circumvent this problem, we slightly relax the constraints by introducing slack variables. It is worth noting that the constraints (34), and (36)-(43) are constraints with an upper bound depending on K_g, and K_r respectively. Consequently, we implement the constraints softening on (33) by

$$\begin{bmatrix} (J_r/2)\omega_{r,min}^2 \\ (J_g/2)\omega_{g,min}^2 \end{bmatrix} - \epsilon \leq \begin{bmatrix} K_r \\ K_g \end{bmatrix} \leq \begin{bmatrix} (J_r/2)\omega_{r,max}^2 \\ (J_g/2)\omega_{g,max}^2 \end{bmatrix} + \epsilon$$

with the minimization of the cost modified to

$$\min_{\underline{u},\epsilon} J_{N_p} + \rho \epsilon^T \epsilon$$

where ϵ, a nonnegative vector of appropriate dimension, is treated as an optimization variable and ρ is a nonnegative scalar. Under the nominal mode, ρ is set to zero but whenever a fault is detected and identified the optimization control problem is reconfigured to the faulty mode by setting ρ to a positive value and by modifying the constraint (34) to

$$P_g(t) \leq \eta_g \sqrt{(2/J_g)K_g(t)}(T_{g,max} - \hat{T}_b). \tag{44}$$

IV. Simulation Results

The proposed FTeMPC scheme is implemented on a nonlinear $2MW$ wind turbine system with detailed ratings of the turbine given in [18]. In these simulations, the turbine is operating at its rated speed (i.e. in region 3 of the power-wind profile) with a wind velocity of $20m/s$ as the mean value. At the rated generator speed, the reference of the kinetic energy is $K_r^{ref} = 10.034MJ$. We solve the convex optimal control problem for eMPC using Yalmip [28] under a Matlab/Simulink environment. The parameters of the wind turbine are given in Table I, whereas the parameters of the eMPC are chosen as

$$h = \Delta\tau_k = 50ms, N_p = 20, \alpha_i = 1, \\ \alpha_j = 100, i = \{1, 5, 6\}, j = \{2, 3, 4\} \tag{45}$$

The bias fault in the converter subsystem with a magnitude of $2000Nm$ is introduced at $t = 500s$. A fault occurring in WT changes the healthy (or fault-free) mode of operation of the turbine to a faulty mode. Since we use a Taylorian linearized model for fault diagnosis, the nonlinear model is linearized around two operating points (OP). These OPs are determined from the closed-loop signals. Let OP_h and OP_f denotes the operating point of the healthy mode and the faulty mode respectively, i.e.,

$$\text{OP}_h \triangleq \begin{cases} u_1^* = \begin{bmatrix} 8845Nm & 21.4deg \end{bmatrix} \\ \breve{y}_1^* = \begin{bmatrix} 226.12rad/s & 2MW \end{bmatrix} \end{cases},$$

$$\text{OP}_f \triangleq \begin{cases} u_2^* = \begin{bmatrix} 8942Nm & 18.7deg \end{bmatrix} \\ \breve{y}_2^* = \begin{bmatrix} 261.82rad/s & 2.4MW \end{bmatrix} \end{cases}.$$

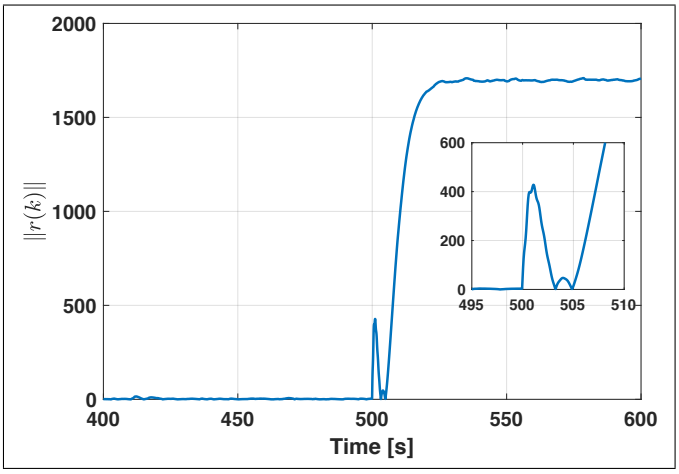

Fig. 3. Norm of the residual signal

TABLE I
Wind turbine parameters

Parameter	Description	Value
ρ	air density	$1.225kg/m^3$
R	radius of the rotor	$33.29m$
β_{min}, β_{max}	constraints on β	$0°, 45°$
$\dot{\beta}_{min}, \dot{\beta}_{max}$	rate constraints on β	$\pm 10°/s$
$\omega_{r,rat}$	rated rotor speed	$3.0408rad/s$
$\omega_{r,min}, \omega_{r,max}$	constraints on ω_r	$0.9, 3.2$
$P_{g,rat}$	rated generated power	$2MW$
J_r	rotor inertia	$1.86 \times 10^6 kgm^2$
J_g	generator inertia	$56.29kgm^2$
K_{dt}	torsion stiffness	$31.8 \times 10^4 Nm/rad$
N_g	gearbox ratio	74.38
κ	converter model parameter	0.02s
K_t	tower equivalent stiffness	$1652000Nm/rad$
B_t	tower equivalent damping	$7589Nm/(rad/s)$
M_t	tower equivalent mass	$54606kg$
h_H	hub height	$31.8 \times 10^4 Nm/rad$

This article has been accepted for publication in a future issue of this journal, but has not been fully edited. Content may change prior to final publication. Citation information: DOI 10.1109/TSTE.2018.2869480, IEEE Transactions on Sustainable Energy

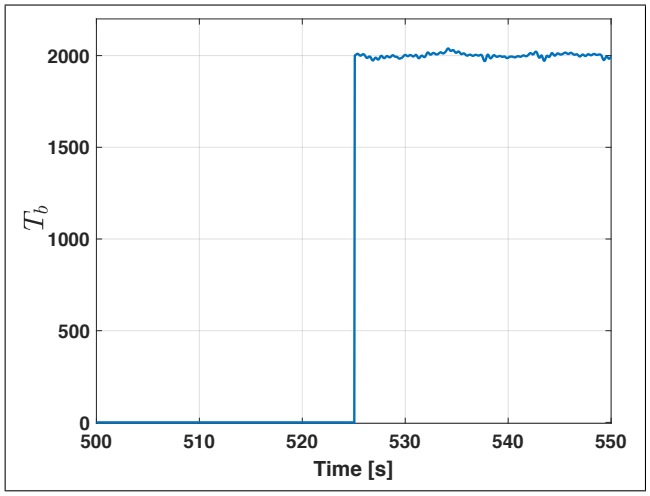

Fig. 4. Estimation of T_b

For fault detection, the eigenvalues of the UIRG (22) are placed inside the unit circle at (0.97,0.97) of the complex plane, and the threshold value in the logic (24) is chosen as 500. The norm of the residual signal generated by the UIRG (22) is shown in Fig. 3 which clearly indicates that the fault is detected at $t = 507.6s$. In the second stage of fault diagnosis, bias estimation is triggered when WT is operating at OP_f. The new steady-state of WT after the occurrence of fault is reached at $t = 525s$. At this time instant, the matrices in (27) are computed around OP_f, which provides the estimation of the bias fault. The estimated bias is illustrated in Fig. 4. Since the fault is estimated at the same time instant, the constraints of the eMPC are reconfigured at $t = 525s$. The closed-loop signals of WT under no fault accommodation and with FTeMPC are illustrated in Fig. 5 by the red curves and the green curves respectively for variables $P_g, TFAM, T_{g,ref}$ and β . The top curve in blue is the mean wind speed profile. It can be seen from the figure that under a bias fault in converter subsystem, the TFAM increases. It is worth observing that the proposed FTeMPC strategy successfully compensates for bias fault and regulates the WT at the rated power with the benefits of achieving an optimal behavior with regards to the economic performance goal.

V. Conclusion

In this paper, we have presented a novel active fault-tolerant control strategy for wind turbines based on economic model predictive control aimed at maximization of system's profitability. The fault diagnosis algorithm of the FTC scheme is built upon an unknown input residual generator and the design of a specific filter which perform respectively detection and estimation of the fault signal. The control algorithm for fault accommodation is achieved by a model predictive control technique resulting from a convex reformulation of the original economic optimization problem along with a particular representation of the WT nonlinear dynamics as a linear dynamics with new decision variables. The effectiveness of the proposed FTeMPC has been demonstrated on a $2MW$ turbine with numerical simulations on a $2MW$ turbine.

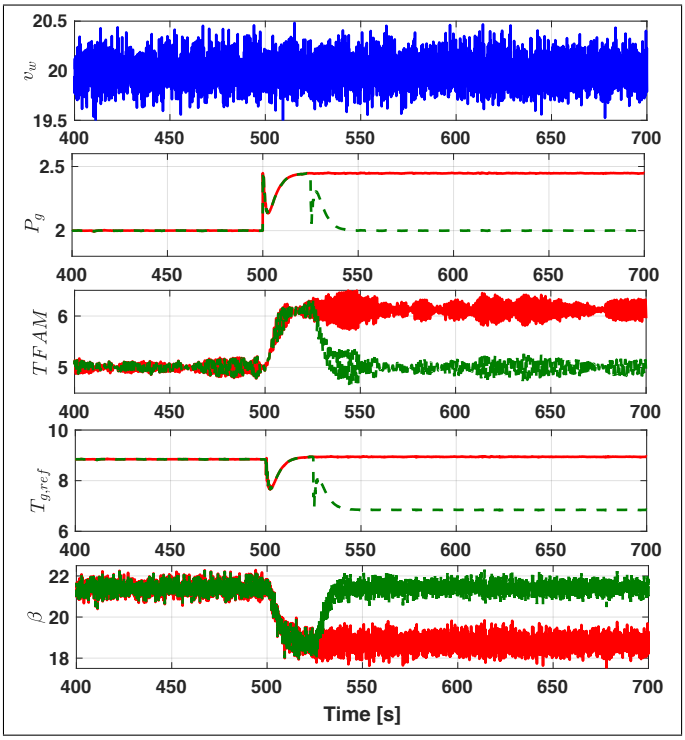

Fig. 5. Closed-loop signals with red/solid line denote the behavior of turbine under no fault accommodation, while signals in green/dashed line denote the WT behavior under FTeMPC. The units of variables v_w, P_g, $TFAM$, $T_{g,ref}$, β are in m/s, MW, MNm, KNm, deg respectively.

Acknowledgment

This research work is supported by the Science & Engineering Research Board (SERB), Government of India under the grant agreement no. ECR/2016/001025.

References

[1] S. De La Saale, D. Reardon, W. Leithead, and M. Grimble, "Review of wind turbine control," *International Journal on Control*, vol. 52, no. 6, pp. 1295–1310, 1990.

[2] L. Pao and K. Johnson, "Control of wind turbines: Approaches, challenges, and recent developments," *IEEE Control Systems Magazine*, vol. 31, no. 2, pp. 44–62, 2011.

[3] F. Bianchi, H. de Battista, and R. Mantz, *Wind Turbine Control Systems: Principles, Modelling and Gain Scheduling Design*. Springer-Verlag London, 2007.

[4] P. Odgaard, J. Stoustrup, and M. Kinnaert, "Fault-tolerant control of wind turbines: A benchmark model," *IEEE Transactions on Control Systems Technology*, vol. 21, no. 4, pp. 1168–1182, 2013.

[5] C. Svärd and M. Nyberg, "Automated design of an FDI system for the wind turbine benchmark," *Journal of Control Science and Engineering*, vol. 2012, p. 13 pages, 2012.

[6] X. Zhang, Q. Zhang, S. Zhao, R. Ferrari, M. Polycarpou, and T. Parisini, "Fault detection and isolation of the wind turbine benchmark: An estimation-based approach," in *IFAC World Congress*, vol. 44, no. 1, 2011, pp. 8295–8300.

[7] D. Rotondo, F. Nejjari, V. Puig, and J. Blesa, "Fault tolerant control of the wind turbine benchmark using virtual sensors/actuators," in *IFAC SafeProcess*, vol. 45, no. 20, 2012, pp. 114–119.

[8] M. Sami and R. Patton, "An FTC approach to wind turbine power maximisation via TS fuzzy modelling and control," in *IFAC SafeProcess*, vol. 45, no. 20, 2012, pp. 349–354.

[9] T. Jain, J. Yamé, and D. Sauter, *Active Fault-Tolerant Control Systems: A Behavioral System Theoretic Perspective*, 1st ed., ser. Studies in Systems, Decision and Control. Springer International Publishing, 2018.

[10] C. Sloth, T. Esbensen, and J. Stoustrup, "Robust and fault-tolerant linear parameter-varying control of wind turbines," *Mechatronics*, vol. 21, no. 4, pp. 645–659, 2011.

[11] T. Jain, J. Yamé, and D. Sauter, "A novel approach to real-time fault accommodation in NREL's 5-MW wind turbine systems," *IEEE Transactions on Sustainable Energy*, vol. 4, no. 4, pp. 1082–1090, 2013.
[12] M. Geyler and P. Caselitz, "Robust multivariable pitch control design for load reduction on large wind turbines," *Journal of solar energy engineering*, vol. 130, no. 3, p. 031014, 2008.
[13] E. Bossanyi, "Wind turbine control for load reduction," *Wind Energy*, vol. 6, no. 3, pp. 229–244, 2003.
[14] M. Mirzaei, M. Soltani, N. K. Poulsen, and H. H. Niemann, "An MPC approach to individual pitch control of wind turbines using uncertain lidar measurements," in *European Control Conference*. IEEE, 2013, pp. 490–495.
[15] M. Soltani, R. Wisniewski, P. Brath, and S. Boyd, "Load reduction of wind turbines using receding horizon control," in *IEEE Multi-Conference on Systems and Control*. IEEE, 2011, pp. 852–857.
[16] S. Gros and A. Schild, "Real-time economic nonlinear model predictive control for wind turbine control," *International Journal of Control*, vol. 90, no. 12, pp. 2799–2812, 2017.
[17] D. Schlipf, D. J. Schlipf, and M. Kühn, "Nonlinear model predictive control of wind turbines using LIDAR," *Wind Energy*, vol. 16, no. 7, pp. 1107–1129, 2013.
[18] M. Soliman, O. P. Malik, and D. T. Westwick, "Multiple model multiple-input multiple-output predictive control for variable speed variable pitch wind energy conversion systems," *IET renewable power generation*, vol. 5, no. 2, pp. 124–136, 2011.
[19] M. A. Benlahrache, S. Othman, and N. Sheibat-Othman, "Fault tolerant control of wind turbine using Laguerre and Kautz MPC for compensation," in *European Control Conference*. IEEE, 2016, pp. 1909–1914.
[20] J. L. Peeters, D. Vandepitte, and P. Sas, "Analysis of internal drive train dynamics in a wind turbine," *Wind Energy*, vol. 9, no. 1-2, pp. 141–161, 2006.
[21] H. Badihi, Y. Zhang, and H. Hong, "Wind turbine fault diagnosis and fault-tolerant torque load control against actuator faults," *IEEE Transactions on Control Systems Technology*, vol. 23, no. 4, pp. 1351–1372, 2015.
[22] D. G. Giaourakis and A. N. Safacas, "Quantitative and qualitative behavior analysis of a dfig wind energy conversion system by a wind gust and converter faults," *Wind Energy*, vol. 19, no. 3, pp. 527–546, 2016.
[23] J. Chen and R. Patton, *Robust Model-Based Fault Diagnosis for Dynamic Systems*. Springer US, 1999.
[24] T. Hovgaard, S. Boyd, and J. Jørgensen, "Model predictive control for wind power gradients," *Wind Energy*, vol. 18, no. 6, pp. 991–1006, 2015.
[25] A. Magnani and S. P. Boyd, "Convex piecewise-linear fitting," *Optimization and Engineering*, vol. 10, no. 1, pp. 1–17, 2009.
[26] M. R. Osborne, *Simplicial Algorithms for Minimizing Polyhedral Functions*. Cambridge University Press, 2000.
[27] J. T. Betts, *Practical methods for optimal control and estimation using nonlinear programming*. Society for Industrial and Applied Mathematics, 2010.
[28] J. Löfberg, "YALMIP : A Toolbox for Modeling and Optimization in MATLAB," in *IEEE International Symposium on Computer Aided Control Systems Design*, 2004, pp. 284–289.